1 The additionality problem of Ocean Alkalinity Enhancement

3 Lennart T. Bach

5 Institute for Marine and Antarctic Studies, University of Tasmania, Hobart, TAS, Australia.

7 *Correspondence to*: Lennart T. Bach (Lennart.bach@utas.edu.au)

10 **Abstract.** Ocean Alkalinity Enhancement (OAE) is an emerging approach for atmospheric carbon dioxide

11 removal (CDR). The net climatic benefit of OAE depends on how much it can increase carbon sequestration

12 relative to a baseline state without OAE. This so-called 'additionality' can be calculated as:

14 $$\text{Additionality} = C_{OAE} - \Delta C_{baseline}$$

16 So far, feasibility studies on OAE have mainly focussed on enhancing alkalinity in the oceans (C_{OAE}) but not

17 primarily how such anthropogenic alkalinity would modify the natural alkalinity cycle ($\Delta C_{baseline}$). Here, I present

18 incubation experiments where materials considered for OAE (sodium hydroxide, steel slag, olivine) are exposed

19 to beach sand to investigate the influence of anthropogenic alkalinity on natural alkalinity sources and sinks. The

20 experiments show that anthropogenic alkalinity can strongly reduce the generation of natural alkalinity, thereby

21 reducing additionality. This is because the anthropogenic alkalinity increases the calcium carbonate saturation

22 state, which reduces the dissolution of calcium carbonate from sand, a natural alkalinity source. I argue that this

23 'additionality problem' of OAE is potentially widespread and applies to many marine systems where OAE

24 implementation is considered – far beyond the beach scenario investigated in this study. However, the problem

25 can potentially be mitigated by dilute dosing of anthropogenic alkalinity into the ocean environment, especially

26 at hotspots of natural alkalinity cycling such as in marine sediments. Understanding a potential slowdown of the

27 natural alkalinity cycle through the introduction of an anthropogenic alkalinity cycle will be crucial for the

28 assessment of OAE.

29

30   **1. Introduction**

31

32 Keeping global warming between 1.5 to 2°C requires rapid reduction of greenhouse gas emissions and gigatonne-

33 scale atmospheric carbon dioxide removal (CDR), using a portfolio of terrestrial and marine CDR methods

34 (Nemet et al., 2018). Ocean alkalinity enhancement (OAE) is considered as an important CDR method of the

35 marine portfolio (Hartmann et al., 2013). OAE can be achieved through a variety of geochemical and

36 electrochemical processes (Renforth and Henderson, 2017). All of them enhance surface ocean alkalinity to

37 reduce the hydrogen ion (H^+) concentration in seawater (i.e. increase pH). This reduction in $[H^+]$ causes a shift in

38 the carbonate chemistry equilibrium:

39

40 $$CO_2 + H_2O \leftrightarrow H^+ + HCO_3^- \leftrightarrow 2H^+ + CO_3^{2-} \qquad (1)$$

42 from CO_2 on the left towards bicarbonate (HCO_3^-) and carbonate ion (CO_3^{2-}) on the right. The associated reduction
43 of the CO_2 partial pressure in seawater (pCO_2) enables atmospheric CO_2 influx into the oceans (or reduces CO_2
44 outflux if pCO_2 > atmospheric pCO_2). This transfer (retention) of atmospheric CO_2 into the ocean leads to an
45 increase of the dissolved inorganic carbon (DIC) concentration in seawater:

47 $$DIC = [CO_2] + [HCO_3^-] + [CO_3^{2-}] \qquad (2)$$

49 Among the widely discussed OAE approaches are coastal enhanced weathering and electrodialytical acid removal
50 (Eisaman et al., 2023). Coastal Enhanced Weathering achieves alkalinity increase via the addition of pulverized
51 alkaline rocks like limestone, olivine, or alkaline industrial products like steel slag to coastal environments (Feng
52 et al., 2017; Harvey, 2008; Meysman and Montserrat, 2017; Renforth, 2019; Schuiling and Krijgsman, 2006). In
53 the case of limestone, alkalinity enhancement and CDR are generated through the dissolution of e.g. $CaCO_3$:

55 $$CaCO_3 + CO_2 + H_2O \rightarrow Ca^{2+} + 2HCO_3^- \qquad (3)$$

57 For olivine, alkalinity enhancement and CDR are driven predominantly by the dissolution of Forsterite (Mg_2SIO_4):

59 $$Mg_2SiO_4 + 4CO_2 + 4H_2O \rightarrow 2Mg^{2+} + 4HCO_3^- + H_4SiO_4 \qquad (4)$$
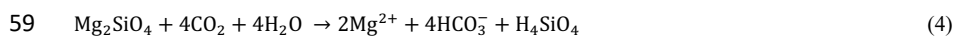
61 For steel slags, the predominant source for alkalinity contained within the material are hydroxides such as calcium
62 oxide (CaO) (Shi, 2004). Here, the net reaction of OAE and associated CDR is:

64 $$CaO + 2CO_2 + H_2O \rightarrow Ca^{2+} + 2HCO_3^- \qquad (5)$$

66 Electrodialytical OAE is somewhat different from the above approaches since no materials are added to
67 seawater. Instead, water is split into H^+ and a hydroxide ion (OH-) using electrical energy and electrodialytic
68 membranes (de Lannoy et al., 2018). H^+ is captured as hydrochloric acid whilst OH- is captured as sodium
69 hydroxide (NaOH). The hydrochloric acid needs to be utilised, neutralized in deep ocean sediments, or stored in
70 save reservoirs outside the ocean (Eisaman et al., 2018; Tyka et al., 2022). NaOH is enriched in the processed
71 seawater, which is released back into the surface convert CO_2 into HCO_3^- (Eisaman et al., 2018; Tyka et al., 2022):

73 $$NaOH + CO_2 \rightarrow Na^+ + HCO_3^- \qquad (6)$$

75 A critical side-effect of OAE is the associated increase in CO_3^{2-} concentrations, which comes through the shift in
76 the marine carbonate equilibrium through H^+ absorption (see above). This increase elevates the saturation state
77 for calcium carbonate (Ω_{CaCO3}), the metric which determines the solubility of $CaCO_3$ in seawater. Ω_{CaCO3} is defined
78 as:
79

80 $$\Omega_{CaCO3} = \frac{[Ca^{2+}]_{SW} \times [CO_3^{2-}]_{SW}}{K_{sp}} \qquad (7)$$

81

82 where $[Ca^{2+}]_{SW}$ and $[CO_3^{2-}]_{SW}$ are calcium ion (Ca^{2+}) and CO_3^{2-} concentration in seawater and K_{sp} is the

83 empirically determined solubility product (Mucci, 1983). K_{sp} differs for different crystal forms of $CaCO_3$. It is

84 higher for Aragonite than for Calcite, meaning Aragonite is more soluble (Mucci, 1983). Aragonite (Ara) and

85 Calcite (Cal) precipitation is thermodynamically favoured when Ω_{Ara} and Ω_{Cal} are ≥ 1. $CaCO_3$ precipitation is of

86 high relevance for the assessment of OAE as the drawdown of CO_3^{2-} through precipitation reduces alkalinity,

87 shifts the carbonate chemistry equilibrium (eq. 1) towards CO_2 and thus counters the CDR efficiency of OAE

88 (Fuhr et al., 2022; Hartmann et al., 2023; Moras et al., 2022).

89   Logistical constraints suggest that OAE would at least initially more likely be conducted in coastal

90 environments (He and Tyka, 2023; Lezaun, 2021; Renforth and Henderson, 2017). Here, alkalinity-enhanced

91 seawater would likely be in contact with marine sediments (Feng et al., 2017; Harvey, 2008; Meysman and

92 Montserrat, 2017). The highly abundant particles in marine sediments can serve as nuclei for $CaCO_3$ precipitation

93 thereby catalysing alkalinity loss when Ω_{CaCO3} is ≥ 1 (Morse et al., 2003; Zhong and Mucci, 1989). This constitutes

94 a problem for OAE because alkalinity-enhanced seawater with its high Ω_{CaCO3} is then exposed to particles that

95 catalyse precipitation. Indeed, recent studies have demonstrated that this particle-catalysed precipitation can

96 rapidly reduce alkalinity, with the degree and rate of alkalinity reduction depending on the amount of alkalinity

97 added and the particle concentrations (Fuhr et al., 2022; Hartmann et al., 2023; Moras et al., 2022).

98 Particle-catalysed $CaCO_3$ precipitation has received significant consideration as a loss term for OAE efficiency

99 (Fuhr et al., 2022; Hartmann et al., 2013, 2023; Moras et al., 2022; Renforth and Henderson, 2017). However,

100 there is another complication associated with OAE near sediments, which has to the best of my knowledge not

101 been considered so far. Sediments can not only provide precipitation nuclei but also constitute natural alkalinity

102 sources, for example via dissolution of $CaCO_3$ or other carbonates.

103   Sandy beaches are often rich in biogenic carbonates. They can also be rich in organic matter thereby

104 creating environments of high respiratory CO_2. Accordingly, Ω_{CaCO3} is low close to the sediments or within pore

105 waters and $CaCO_3$ dissolution is favoured (Liu et al., 2021; Perkins et al., 2022; Reckhardt et al., 2015). This form

106 of natural alkalinity formation via $CaCO_3$ dissolution sequesters respired CO_2 which may have otherwise be

107 released into the atmosphere (Aller, 1982; Fakhraee et al., 2023; Krumins et al., 2013; Saderne et al., 2021). OAE

108 within these naturally low Ω_{CaCO3} environments could have two effects. First, it would have the desired effect of

109 consuming H^+ and increasing CO_2 sequestration via the generation of anthropogenic alkalinity (eqs. 2-4). Second,

110 the consumption of H^+ would increase Ω_{CaCO3}, which could reduce the dissolution of $CaCO_3$ and thus reduce

111 natural CO_2 sequestration since less natural alkalinity is produced. Due to this second effect, the first (desired)

112 effect of CO_2 sequestration may be significantly reduced. Accordingly, the net gain in CO_2 sequestration would

113 be lower than one would have hoped for.

114   The concept "additionality" describes the net gain in CO_2 sequestration achieved through the

115 implementation of a CDR method. It can be defined in simple terms as:

116

117 $$\text{Additionality} = C_{OAE} - \Delta C_{baseline} \qquad (8)$$

118

119   where C_{OAE} is the CO_2 sequestration achieved through OAE, and $\Delta C_{baseline}$ is the change in the baseline CO_2
120   sequestration through the implementation of OAE.

121   This study aims to reveal and describe how anthropogenic alkalinity affects natural alkalinity release. I
122   present some observational data and three experiments where 3 types of anthropogenic alkalinity sources (NaOH,
123   steel slag, olivine) are exposed to a natural alkalinity source and sink (beach sand) to investigate their interactions.
124   Afterwards, I examine these interactions (termed "additionality problem"), discuss their relevance, and how it
125   could be mitigated.

126

2.   Methods

127
128

2.1. Carbonate chemistry and dissolved silicate transects along Southern Tasmanian beaches

129
130

131   The project was initialised with near-shore alkalinity, pH, and dissolved silicate (DSi) transects from the swash
132   zone to ~200 m offshore on 4 beach locations (Clifton South, Clifton North, Goats, Wedge) near Hobart
133   (Tasmania). Goal of these transects was to determine whether the beaches are detectable alkalinity sinks or sources
134   and to inform the incubation experiments. An overview of the sampled beaches with approximate conditions and
135   exact coordinates is provided in Table S1 and Fig. S1.

136   Samples for alkalinity and DSi were taken by filling 200 mL seawater from 0.2 m depth into a
137   polyethylene (PE) bottle. Samples for pH were collected in a 60 mL polystyrene (PS) jars filled and closed at 0.2
138   m depth. Both the PE bottles and the PS jars were pre-rinsed with sample. The sample closest to shore was taken
139   in the swash zone at the spot where a wave reached highest within ~5 minutes of observation. A ~0.2 m deep hole
140   was dug (Fig. S1) and water was collected from the groundwater with a 60 mL syringe. The second sample was
141   from the upper part of the swash zone where waves pushed water up the beach. Samples further out were taken
142   from within the wave breaking zone to about 50-100 m beyond the wave breaking zone. Samples were taken by
143   walking into the water to the point it became too deep and a surfboard was used as sampling vehicle.

144   The samples were transported back to the beach where pH was measured immediately (i.e. within 15
145   minutes after sampling) as described in section 2.4. Alkalinity and DSi samples were filtered after pH
146   measurements with a 0.22 syringe filter (nylon membrane) into a 125 mL PE bottle (alkalinity) or 60 mL PS
147   plastic jar (DSi). Both containers, the syringe, and the syringe filter were pre-rinsed with sample.

148

2.2. Laboratory experiments

149
150

2.2.1.   Experiment 1: Replicated mineral dissolution assays to monitor interaction between
           beach sand and weathering minerals

151
152
153

154   Experiment 1 was designed to investigate the interaction between 4 different beach sands and alkaline minerals
155   during the incubation in seawater. The experiment required 60 HDPE bottles, each with a volume of 125 mL.
156   These 60 bottles were thoroughly cleaned with double-deionised water and dried at 60°C. Twelve bottles were
157   filled with sand from one of the 4 sampling locations (section 2.3.), respectively (totalling 48 bottles). Another
158   set of 12 bottles were not filled with sand. This yielded 5 sets of 12 bottles (Fig. 1). Of each set, 3 bottles remained

159   without further addition, 3 received 51.3 µL of 1 molar NaOH, 3 received 0.0065 g of ground steel slag, and 3

160   received 1 g of ground olivine (Fig. 1; sand, steel slag, and olivine properties were determined as described in

161   section 2.3.). The 48 bottles that contained sand were filled with 10 g of sand if slag or NaOH was added or 9 g

162   of sand if olivine was added. This was done so that the weights of added sand plus alkalinity feedstock was always

163   ~10 g.

164   Once the solid components were added, each bottle was filled with 120 (+/-4) g of seawater (S=35 ±2, alkalinity

165   = 2259.7 µmol/kg) collected in July 2022 in the Derwent Estuary near Taroona. Salinity and pH of the seawater

166   was determined a few minutes before transfer into the incubation bottles with a Metrohm 914 pH/conductivty

167   meter as described in section 2.4. The transfer of the seawater into the incubation bottles took 30 minutes in total

168   (please note that in the case of NaOH additions, seawater was added to the bottles before 51.3 µL of 1 molar

169   NaOH was added). The incubation bottles were immediately mounted on plankton wheel (1.06 m diameter, 2

170   rounds per minute), which was placed in a temperature-controlled room set to 15°C (Fig. S2). The plankton wheel

171   kept the various mixtures of sand, alkalinity source, and seawater moving inside the bottles. The experiment

172   commenced at 16:00 on the 17th of August, 2022.

173   After ~6.8 days (24th of August), bottles were consecutively removed from the plankton wheel in random order

174   between 8:00 and 15:30. pH was measured inside the bottle with a pH electrode, directly after a bottle was taken

175   off the plankton wheel. Afterwards, the alkalinity sample was filtered with a syringe through a 0.2 µm nylon filter

176   into a dry and clean 125 mL HDPE bottle and stored in the dark at 7°C.

177

178   **2.2.2.   Experiment 2: Alkalinity formation at Omega gradients**

179

180   Experiment 2 was designed to investigate whether a decline of Ω_{CaCO_3} enhances the formation of natural alkalinity

181   via $CaCO_3$ dissolution and how anthropogenic alkalinity sources (olivine, slag, NaOH) influence this process. The

182   experiment required 60 HDPE bottles (125 mL) cleaned with acid and double-deionised water (note that acid was

183   used in Experiment 2 to make sure all remnants from Experiment 1 were washed out of the bottles). All 60

184   incubation bottles were filled with sand from Clifton Beach (section 2.4.). The treatments were then set up as

185   follows: Twelve bottles were filled only with 10 g of sand; Twelve with 10 g of sand and 0.006515 (+/-0.00007)

186   g steel slag; Twelve with 9 g of sand and 1 (+/-0.002) g of olivine; Eight with 10 g of sand at "un-equilibrated"

187   NaOH addition; Sixteen with 10 g of sand at "equilibrated" NaOH addition (Fig. 1).

188   For each treatment, a gradient in seawater CO_2 concentrations was established from bottle 1 (lowest CO_2) to bottle

189   8-16 (highest CO_2). This was achieved with the following approach: A batch of seawater (S= 35±0.2, alkalinity =

190   2266.8 µmol/kg) was collected in November 2022 in the Derwent Estuary near Taroona. About 0.3L of the batch

191   was bubbled with pure CO_2 gas for about 5 minutes to generate highly CO_2-enriched seawater. Another ~7L of

192   the batch was used as source water to fill the incubation bottles. pH and temperature were measured in this batch

193   prior to filling the incubation bottles. The low CO_2 incubation bottles (bottle 1 in the sequence from e.g. 1 to 12,

194   Fig. 1) were then filled first. Afterwards, about 20 mL of the CO_2-enriched water was added to the batch, shaken

195   thoroughly to mix it and the pH and temperature were measured again. Once a stable pH/temperature reading was

196   achieved, the next bottles (bottle 2) were filled. This procedure was repeated until all bottles in a treatment were

197   filled with an increasing CO_2 concentration. For the equilibrated and un-equilibrated NaOH treatments, I followed

198   the same procedure but separate 0.3L and 7L batches were used for the CO_2 enrichment that had previously been

199   amended with NaOH to elevate alkalinity from 2266.8 to 2757.4 µmol/kg prior to filling the incubation bottles.

200   All 60 bottles were filled with 120 +/-4 g of seawater and immediately mounted on the plankton wheel (2nd of

201   December, 2022; 17:00) under the same conditions as in Experiment 1 (i.e. 15°C, 2 rounds per minute, Fig. S2).

202   After ~6.8 days (9th of December), bottles were removed from the plankton wheel between 9:00 and 16:00. pH

203   and alkalinity were sampled as described in section 2.2.1.

204

205   **2.2.3.**   **Experiment 3: pH dependency of alkalinity formation from slag and olivine**

206

207   Experiment 3 was designed to investigate whether a lower seawater pH would promote alkalinity formation from

208   steel slag and olivine.

209   The experiment required 12 new HDPE bottles (125 mL) cleaned with double-deionised water and dried

210   thereafter. Six of the 12 bottles were filled with 0.00644 (±0.00007) g steel slag and the other six with 1.0003

211   (±0.002) g of olivine. Three slag and three olivine bottles were filled with seawater from the same seawater source

212   as used in Experiment 2 (S=35±0.2, alkalinity=2263.2 µmol/kg, pH_T = 7.82). pH and temperature were measured

213   prior to filling the bottles with seawater (section 2.4.). Afterwards, the ~2L seawater batch was amended with

214   about 80 mL of CO_2-enriched seawater as explained in section 2.2.2. This enrichment lowered the pH_T (total

215   scale) from 7.82 to 6.846. This low pH_T (high CO_2) seawater was used to fill the other 3 slag and olivine incubation

216   bottles. The 12 bottles with 122.8 (±0.15) g of seawater were immediately mounted on the plankton wheel (Fig.

217   S2) after filling (16th of December, 2022; 16:40) under the same conditions as in Experiment 1 and 2 (i.e. 15°C,

218   2 rounds per minute).

219   After ~6.8 days (23rd of December), the 12 bottles were randomly removed from the plankton wheel between 9:00

220   and 11:00. pH and alkalinity were sampled as described in section 2.2.1.

221
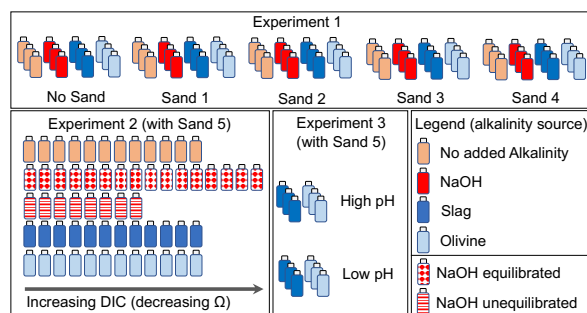
223   **Figure 1**. Design of Experiments 1, 2, and 3. Bottles represent treatments with incubation of seawater, sand, and

224   alkalinity sources (color code represents alkalinity source). In Experiment 2, NaOH was used as alkalinity source

225   in two explicit scenarios as described in section 2.2.2.

226

227   **2.3. Preparation and characterization of weathering minerals and beach sand**

228

229   In total, 5 sand samples (0.5-1kg) were collected for Experiments 1 and 2 at Clifton Beach, Tasmania (Fig. S1,

230   Table S1). Sampling permission was granted by the Department of Natural Resources and Environment (Authority

231   No. ES 22314). Wet sand was sampled on the upper end of the swash zone and stored in zip bags at 15°C. Samples

232   1-4 were used for Experiment 1, ~24 hours after sampling while sample 5 was used for Experiment 2, ~72 hours

233   after sampling.

234   Olivine rocks were sourced from the Mount Shadwell Quarry in Mortlake (Australia, Table S1). Basic oxygen

235   slag (hereafter just called slag) was sourced from the Liberty Primary Steel – Whyalla Steelworks (Australia,

236   Table S1). Olivine rocks and slag (Fig. S3) were crushed with a hydraulic crusher into smaller pieces of about 10

237   mm and then milled with a ring mill in a chrome milling pot. Milled slag and olivine were sieved, first with a 250

238   μm sieve and then with a 150 μm sieve. The fractions retained on the 150 μm sieve were used for experiments.

239   Wet and dry weight of the sand used for laboratory experiments was determined by weight difference of a wet

240   and a dry sample. The wet sample (~80 g) was put into a clean plastic jar and dried for 24-72 hours. The particle

241   size spectra of the 5 dried sand samples as well as slag and olivine mineral were determined with a Sympatec

242   QICPIC particle imager.

243   For total particulate carbon (TPC) and particulate organic carbon (POC) analyses, dried sand samples were milled

244   for 12 minutes in a Retsch MM200 ball mill. Between 4-10 mg of each of the pulverized sand samples were

245   weighed into 10 tin cups for TPC or 10 silver cups for POC (2 TPC and POC replicates for each sample). The

246   POC samples were moisturized with 50μL of MilliQ water, placed for 18 hours in a dessicator that contained 36%

247   HCl to remove all carbonates and then dried. TPC and POC samples were analysed for carbon content using a

248   Thermo Finnigan EA 1112 Series Flash Elemental Analyser. Particulate inorganic carbon (PIC) content of the

249   samples was then calculated as the difference between TPC and POC. Percent content of carbonates was estimated

250   by multiplying % PIC content by the molecular weight of $CaCO_3$ (100 g/mol) and $MgCO_3$ (84.3 g/mol) for upper

251   and lower estimates.

252

253   **2.4. Carbonate chemistry, salinity, and dissolved silicate measurements**

254

255   pH was determined potentiometrically using a Metrohm 914 pH meter following Standard Operation Procedure

256   6a described in (Dickson et al., 2007) but omitting the test for ideal Nernst behaviour of the electrode (ideal Nernst

257   behaviour was assumed). A new pH electrode (Metrohm Aquatrode Plus) was calibrated on the total pH scale

258   (pH_T) with certified reference material (CRM) TRIS buffer (batch #37), provided by Prof. Andrew Dickson's

259   laboratory. The calibration procedure for the relevant temperature range (~8 – 18°C) followed the exact workflow

260   as described by (Ferderer et al., 2022). Precision of the pH measurement was assumed to be ±0.015 based on

261   experience with the probe.

262   alkalinity was determined in an open cell titration following (Dickson et al., 2003). Samples were measured in

263   duplicate with a Metrohm 811 titration unit equipped with a Metrohm Aquatrode Plus. Alkalinity was calculated

264   from titration curves using the Calkulate function of PyCO2sys (Humphreys et al., 2020). The difference in

265   alkalinity between duplicate titrations of the sample was on average 1.95 μmol/kg and >75% were within 4

266   μmol/kg (N=185), which was assumed to be the precision of the measurement (±2 μmol/kg). Accuracy was

267   controlled by correcting alkalinity values with CRM provided by A.G. Dickson's laboratory. Alkalinity was

268   measured within maximally 20 days after sampling.

269   Salinity was measured with a Metrohm conductivity probe with a PT1000 temperature sensor connected to a

270   Metrohm 914 conductivity meter. The probe was calibrated with DIC/alkalinity CRM from A.G. Dickson's

271   laboratory for which a salinity of 33.464 has been reported (CRM batch 200). Conductivity was measured in

272 mS/cm^2 and salinity was subsequently calculated on the practical salinity scale following Lewis and Perkins

273 (1978), following the workflow described by (Moras et al., 2022). A relatively low precision of +/- 0.2 was

274 determined from repeat measurements.

275 Si concentrations for beach transects were measured 18 hours after sampling following Hansen and Koroleff

276 (1999). No Si measurements were conducted for Experiments 1-3.

2.5. Carbonate chemistry calculations

280 Carbonate chemistry conditions were calculated with the "carb function" in Seacarb (Gattuso et al., 2021), with

281 pH_T, alkalinity, salinity, temperature, phosphate and silicate concentrations as input variables, stoichiometric

282 equilibrium constants from Lueker et al. (2000), and default settings for the other equilibrium constants. Si was

283 not measured due to volume limitations so I assumed a values of 50 µmol/kg at the end of the experiments, when

284 either sand, olivine, or slag were incubated. Likewise, phosphate was not measured and I assumed 2 µmol/kg at

285 the end of the experiments when slag was incubated. These Si and phosphate releases were based upon previous

286 trials. Note, however, that concentrations of Si and phosphate within these ranges have negligible impact on

287 calculated carbonate chemistry parameters (e.g. pCO_2 changes by ~1 µatm when Si is assumed to be 0 instead of

288 50 µmol/kg).

289 Propagated errors in derived carbonate chemistry parameters (e.g., DIC) were calculated with the

290 "errors" function in Seacarb using measurement precisions described in section 2.4. for pH (±0.015), alkalinity

291 (±2 µmol/kg), and salinity (±0.2), default uncertainties for equilibrium constants and temperature, and when

292 applicable (see above) ±50 µmol/kg for silicate and ±2 µmol/kg for phosphate.

2.6. Calculations of the CO_2 uptake ratio (η_{CO2}) for carbonate and non-carbonate alkalinity sources

297 The atmospheric CO_2 uptake ratio for OAE (η_{CO2}) was defined as the number of moles DIC absorbed per number

298 of moles alkalinity added (Tyka et al., 2022). η_{CO2} was shown to range roughly between 0.75 and 0.9 mol:mol in

299 the surface ocean (Schulz et al., 2023; Tyka et al., 2022). However, this η_{CO2} range only applies for alkalinity

300 source materials that exclusively increase alkalinity without a concomitant increase in DIC when they are added

301 to seawater ($Alk_{non-carbonate}$). Such sources comprise for example NaOH, slag, and olivine. The estimated range

302 does not apply when all or fractions of the added alkalinity comes from carbonates ($Alk_{carbonate}$), since $CaCO_3$

303 dissolution contributes 2 moles of alkalinity and 1 mole of (non-atmospheric) DIC when they dissolve.

304 The dependency of η_{CO2} on the relative contribution of $Alk_{carbonate}$ and $Alk_{non-carbonate}$ was calculated as:

306 $$\eta_{CO2} = \frac{DIC_{equilibrated} - \left(\frac{Alk_{carbonate}}{2}\right) - DIC_{initial}}{Alk_{non-carbonate} + Alk_{carbonate} - Alk_{initial}} \tag{9}$$

308 Where $DIC_{initial}$ and $Alk_{initial}$ are DIC and alkalinity in seawater before alkalinity was increased, assuming a

309 seawater pCO_2 in equilibration with the atmosphere. $DIC_{equilibrated}$ is the amount of DIC from the environment (e.g.

310 from the atmosphere) that can be stored in seawater after the increase of $Alk_{carbonate}$ and $Alk_{non-carbonate}$, assuming

311   seawater pCO_2 in equilibrium with the atmosphere. η_{CO2} was first calculated for a theoretical case where $Alk_{initial}$

312   was 2350 µmol/kg and $DIC_{initial}$ was calculated for the surface ocean (15°C, S = 35, carbonate chemistry constants

313   as in section 2.5), assuming a pCO_2 of 420 µatm. $Alk_{carbonate}$ and $Alk_{non-carbonate}$ were then varied in a range of

314   scenarios (from 0 to 100% $Alk_{carbonate}$) to increase the sum of them by 1 µmol/kg. η_{CO2} was calculated for each

315   scenario.

316   Next, η_{CO2} was calculated specifically for Experiment 1 as follows: The increase of alkalinity (ΔAlkalinity) was

317   higher in the NaOH and slag treatments when no sand was present compared to incubations with sand (section

318   3.2). ΔAlkalinity was very likely $Alk_{non-carbonate}$ in all incubations while the reduced ΔAlkalinity in the incubations

319   with sand was likely due to secondary precipitation of carbonates (section 4.2.1). Based on these conclusions,

320   η_{CO2} was estimated as:

321

322    $$\eta_{CO2} = \frac{(\Delta Alkalinity_{no-sand} - \Delta Alkalinity_{sand}) \times 0.5 + \Delta Alkalinity_{sand} \times 0.86}{\Delta Alkalinity_{no-sand}} \qquad (10)$$

323

324   where ΔAlkalinity$_{no-sand}$ and ΔAlkalinity$_{sand}$ are the changes in alkalinity measured in incubations without sand and

325   with sand, respectively; 0.5 is the η_{CO2} when $Alk_{non-carbonate}$ is lost via the precipitation of carbonates where 2 moles

326   of alkalinity and 1 mol of DIC are sequestered; 0.86 is the η_{CO2} when all ΔAlkalinity is $Alk_{non-carbonate}$ under the

327   conditions set up in the experiments (i.e. 15°C, S=35; see above). Please note that ΔAlkalinity was higher in the

328   olivine incubations when sand was present, which is opposite to the NaOH and slag incubations for reasons

329   discussed in section 4.2.1. Therefore, η_{CO2} was calculated assuming all ΔAlkalinity was $Alk_{non-carbonate}$ for the

330   olivine incubations (i.e. η_{CO2} = 0.86). For the incubations without an added alkalinity source all ΔAlkalinity was

331   assumed to be $Alk_{carbonate}$ so that η_{CO2} was 0.36.

332   η_{CO2} was also specifically calculated for Experiment 2. This required knowledge of how much of the measured

333   ΔAlkalinity was contributed by $Alk_{carbonate}$ and $Alk_{non-carbonate}$. In the treatments where only sand was incubated,

334   alkalinity and DIC increased roughly in a 2:1 molar ratio over the course of the experiment (i.e. ΔAlkalinity:ΔDIC

335   = 2:1 mol:mol). Thus, it can be assumed that the vast majority of the measured alkalinity increase is $Alk_{carbonate}$.

336   In contrast, when sand was incubated with alkaline materials, alkalinity and DIC generally increased with a molar

337   ratio that was >2:1 because alkaline materials release alkalinity without a concomitant increase of DIC. Based on

338   these constraints, we can roughly approximate the contribution of $Alk_{carbonate}$ and $Alk_{non-carbonate}$ to the measured

339   alkalinity increase (ΔAlkalinity) as:

340

341    $$\% Alk_{carbonate} = 1 : \left(\left(\frac{\Delta Alkalinity}{\Delta DIC} \right) / 2 \right) \times 100 \qquad (11)$$

342

343   Where $\% Alk_{carbonate}$ is the percentage contribution of $Alk_{carbonate}$ to ΔAlkalinity. Based on eq. (11), a

344   ΔAlkalinity:ΔDIC of for example 8:1 mol:mol would suggest that 25% of the ΔAlkalinity is $Alk_{carbonate}$ and the

345   other 75% $Alk_{non-carbonate}$. $Alk_{carbonate}$ and $Alk_{non-carbonate}$ were calculated with eq. 11 for all incubations in Experiment

346   2 and this information was then used to calculate η_{CO2} with eq. (10). Finally, the amount of DIC that can be stored

347   in seawater due to an increase of $Alk_{carbonate}$ and $Alk_{non-carbonate}$ (DIC_{OAE}) was calculated as:

348

349   $DIC_{OAE} = \eta_{CO2} * \Delta\text{Alkalinity}$ (12)

350

351   for experiments 1 and 2.

352

353   **2.7. Statistical analysis**

354

355   Experiment 1 and 3 were analysed with a two-way analysis of variance (ANOVA) where either "sand" and

356   "alkalinity source material" (Experiment 1) or "carbonate chemistry" and "alkalinity source material"

357   (Experiment 3) were defined as independent variables. The dependent variables were the changes in carbonate

358   chemistry (e.g. ΔAlkalinity) over the course of the incubations. Homogeneity of variance was assessed by visually

359   inspecting if plotted model residuals vs. fitted values is scattering similarly around 0. Normality of the residuals

360   was assessed by inspecting qqplots where theoretical quantiles plotted against standardized residuals should

361   ideally resemble a straight line. Such a straight-line appearance (i.e. ideal normality) was not always given, so

362   some datasets were rank-transformed. However, transformation did not improve normality substantially so that

363   non-transformed data was used for all analyses. Statistical differences between individual treatments were

364   assessed with a Tukey post-hoc. Significant differences were assumed when $p<0.05$.

365   Experiment 2 was analysed by plotting ΔAlkalinity for each alkalinity source material and sand against the

366   increase in DIC that was established via additions of CO_2-saturated seawater (section 2.2.2). The data was fitted

367   with the polynomial equation $a*x^2+bx+c$, where x is the amount of DIC added to each treatment and a, b, c are

368   fit parameters. The curve fitted to the treatments where only sand was added was compared to the curves fitted to

369   the treatments where sand and a certain alkalinity source were added.

370

371   **3. Results**

372

373   **3.1. Beach transects**

374

375   Beach transects consisted of 8-9 sampling points from the just above the swash zone to 150-220 m offshore at

376   four locations (Table S1, Fig. S1). Alkalinity showed distinct patterns across the locations. At Clifton South and

377   Wedge, alkalinity was higher in the swash zone than in the open water. This was particularly pronounced at Clifton

378   South with a value of 2418 µmol/kg relative to open water values of about 2300 µmol/kg (Fig. 2A). At Goats

379   Beach, no such alkalinity gradient was observed across the transect, while alkalinity was lower in the swash zone

380   at Clifton North (Fig. 2A). Wedge differed to the other locations in that alkalinity was generally lower (~2160

381   compared to ~2300 µmol/kg in open water).

382   pH_T was lowest in samples just above the swash zone at all four locations (Fig. 2B). The difference relative to

383   open water was most pronounced at Clifton South with pH_T of 7.76 just above the swash zone compared to

384   approximately 8.05 in the open water, while least pronounced at Goats. Gradients at Clifton North and Wedge

385   were in between these two extremes. pH_T at Wedge was on average higher in the open water than at the other

386   locations, i.e. 8.08 compared to 8.05 (Fig. 2B).

387   $Si(OH)_4$ concentrations were highest in samples from just above the swash zone at all four locations (Fig. 2C).

388   The most pronounced gradient was observed at Clifton South, with $Si(OH)_4$ of 8.6 µmol/L just above the swash

389   zone and ~1.6 µmol/L in open water. The least pronounced gradient was observed at Goats, and intermediate

390   gradients at Clifton North and Wedge (Fig. 2C).

391   Overall, the data shows consistency across the three parameters measured in that Clifton South showed most

392   pronounced trends, Goats the least pronounced trends, and Clifton North and Wedge being in between (Fig. 2).
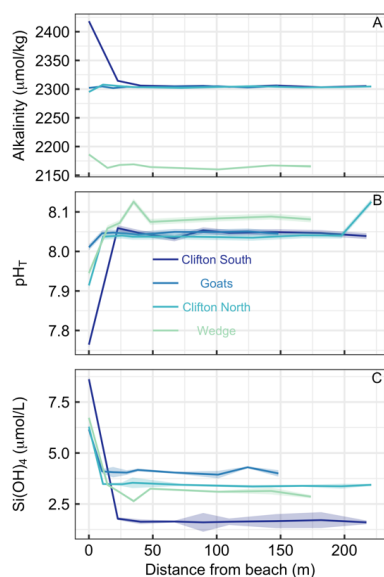
393

394   **Figure 2**. Transects of (A) alkalinity, (B) pH_T, and (C) $SiOH_4$ at four different beach locations in southern

395   Tasmania (see Table S1 and Fig. S1 for locations). The first sampling was at the upper end of the swash zone and

396   then 7-8 more samples were taken until 150-200 m offshore. Lines and shaded areas show averages and

397   uncertainties, respectively.

398

399   **3.2. Experiment 1**

400

401   Alkalinity increased over the course of the 6.8 days in all treatments where alkaline materials were added (Fig.

402   3). Changes in alkalinity (ΔAlkalinity) were between ~610-400 µmol/kg for the slag, ~420-290 µmol/kg for the

403   NaOH, and 280-370 µmol/kg for the olivine treatment. In contrast, ΔAlkalinity changed very little (i.e. ΔAkalinity

404   ≤6 µmol/kg) when no alkaline materials were added. (Please note that an important outlier was observed in Sand

405   2 where ΔAlkalinity was 87.3 µmol/kg which will be discussed in section 4.3.). The two-way ANOVA revealed

406   significant effects of (1) the type of sand, (2) the type of alkalinity source, and (3) the interaction of these two on

407   ΔAlkalinity ($p < 0.05$). For the slag and the NaOH treatment, ΔAlkalinity was significantly higher when these were

408   incubated with no sand but only small differences were observed across the four sand samples. In contrast,

409   ΔAlkalinity was slightly lower in the olivine treatment when no sand was present during incubations although the

410   difference was only significant relative to olivine incubated in Sand 4 (Fig. 3A).

411   Changes in pH_T (ΔpH_T) reflected the patterns described for ΔAlkalinity (Fig. 3B). ΔpH_T was highest in the slag

412   and the NaOH treatment when no sand was added, while this difference between the presence and absence of sand

413   was not observed for olivine. ΔpH_T was slightly negative in treatments where no alkalinity source was added to

414   the incubated sand samples. The two-way ANOVA revealed significant effects of sand, alkalinity source and their

415   interaction on ΔpH_T (p<0.05).

416   η_{CO_2} was prescribed to be 0.36 when sand without an anthropogenic alkalinity source was incubated and 0.86 for

417   olivine incubations (see section 2.6). Calculated η_{CO_2} for NaOH and slag treatments were slightly lower due to

418   relatively lower ΔAlkalinity in the presence of sand than without the presence of sand (Fig 3C). This relatively

419   lower ΔAlkalinity was most likely due to some of the ΔAlkalinity was lost due to secondary precipitation of

420   carbonates. Statistics are not provided for η_{CO_2} data because assumptions of the ANOVA model were heavily

421   violated.

422
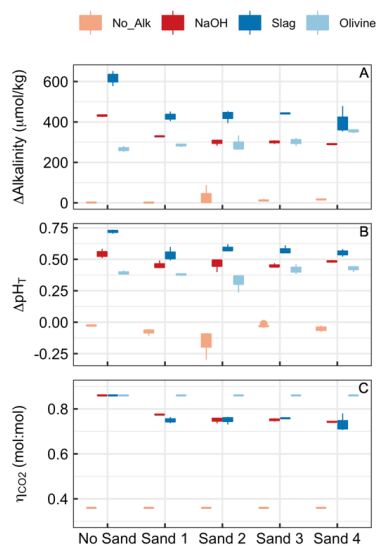
424   **Figure 3**. Results of Experiment 1. Changes of (A) alkalinity and (B) pH_T from the beginning to the end of the

425   6.8 days experiment. (C) η_{CO_2} at the end of the experiment. Boxplots are based on three replicates per treatment.

426   Colours refer to the added alkalinity source (No_Alk means no alkalinity source was added). The alignment on

427   the x-Axis indicates if or which sand sample was present in the incubation bottles ("No Sand" means no Sand was

428   added).

429

430   **3.3. Experiment 2**

431

432   The additions of CO_2-enriched seawater established a gradient of increasing DIC and accordingly a decline in

433   pH_T and Ω_{Ara}. The rationale for this setup was that beach sediments can contain high amounts of respiratory CO_2

434   so that anthropogenic alkalinity added to beaches has a high likelihood to be exposed to such high CO_2 conditions

435   (Liu et al., 2021; Perkins et al., 2022; Reckhardt et al., 2015). Fig. 4 shows ΔAlkalinity along the DIC gradient

436   for different alkalinity source materials (NaOH, slag, olivine) and compares this to ΔAlkalinity along the same

437   DIC gradient where only sand from a beach was present. The "sand only" data is identical in all four plots (orange

438   lines in Fig. 4). It shows that ΔAlkalinity is close to zero in the sand-only incubations when no DIC is added but

439   increases exponentially with increasing DIC additions up to 537 µmol/kg.

440 OAE via NaOH additions was set up in two different scenarios (Fig. 4A, B). In the first scenario, the carbonate

441 system was equilibrated with atmospheric CO_2 after the NaOH deployment and before exposed to the sand (Fig.

442 4A). This setup leads to a gradient in Ω_{Ara} from 2.1 to 0.2 along the DIC gradient at the beginning of the 6.8 days

443 incubations (highest Ω_{Ara} at the lowest DIC addition). In the second scenario, the carbonate system was not

444 equilibrated, thereby assuming that a NaOH-enriched patch of seawater would be exposed to sand sediments

445 before it had taken up atmospheric CO_2 (Fig. 4B). Here, initial Ω_{Ara} ranges from 7.1 to 2.3 along the DIC gradient.

446 In the equilibrated scenario, ΔAlkalinity was 482 µmol/kg when no DIC was added and increased exponentially

447 to 973 µmol/kg at the highest DIC addition (Fig. 4A). In the unequilibrated scenario, ΔAlkalinity was 344 µmol/kg

448 when no DIC was added and increased to 474 µmol/kg at the highest DIC addition. However, in contrast to the

449 equilibrated treatment, the ΔAlkalinity increase weakened along the DIC gradient and ΔAlkalinity was lower than

450 in the sand-only treatment when the DIC addition was >400 µmol/kg (Fig. 4B).

451 In the slag treatment, ΔAlkalinity was 521 µmol/kg when no DIC was added. ΔAlkalinity increased exponentially

452 along the DIC gradient to 814 µmol/kg. The increase of ΔAlkalinity was less pronounced than in the sand-only

453 treatment. Overall, the slag data showed more scatter relative to the other alkalinity source materials and sand-

454 only treatments (Fig. 4C).

455 In the olivine treatment, ΔAlkalinity was 258 µmol/kg when no DIC was added. ΔAlkalinity increased

456 exponentially with increasing DIC additions to 453 µmol/kg although much less pronounced than in the sand-

457 only treatment. ΔAlkalinity was lower in the olivine than in the sand-only treatment when DIC additions were

458 >350 µmol/kg (Fig. 4C).

459
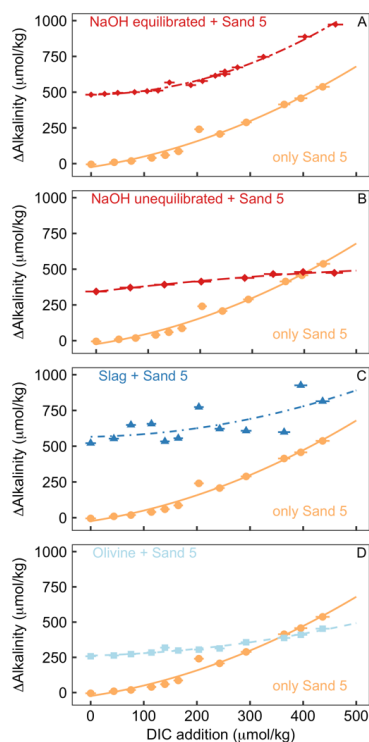
460

461 **Figure 4**. Results of Experiment 2. All panels show the change in alkalinity from the beginning to the end of the
462 6.8 days experiment along a gradient of DIC added to the incubation bottles at the start of the incubations. The
463 orange data displayed on all panels show ΔAlkalinity for incubations where only sand was incubated. The other
464 data on each panel show ΔAlkalinity when sand was incubated with an external alkalinity source or addition
465 scenario. (A) Sand and NaOH equilibrated with atmospheric CO_2 upon addition; (B) Sand and NaOH which was
466 not equilibrated with atmospheric CO_2 upon addition; (C) Sand and slag; (D) Sand and olivine.

467

468 **3.4.** Experiment 3

469

470 Experiment 3 tested if there is a pH dependency of alkalinity release by olivine and slag (Fig. 5). The two-way
471 ANOVA revealed a significant influence of pH_T on the release of alkalinity from olivine and slag (Fig. 4). Slag
472 released 707 ±61 µmol/kg alkalinity when incubated within a pH_T from initially 7.82 to 8.67 at the end of the 6.8
473 days incubation. Within the lower pH_T range from 6.86-8.39, slag released 805 ±86 µmol/kg. Olivine released
474 234 ±36 µmol/kg within the high pH_T range from 7.82-8.20 and 298 ±8 µmol/kg in the low pH_T range from 6.86-
475 7.63 (Fig. 5).

476
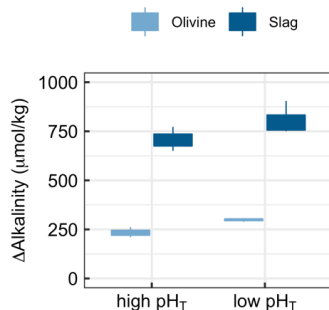
477
478 **Figure 5**. Results of Experiment 3. Changes in alkalinity from the beginning to the end of the 6.8 days experiment
479 when olivine or slag were incubated (without sand) under high (initially 7.82) or low pH_T (initially 6.85).
480 ΔAlkalinity was significantly higher under low pH_T.

481

482 **4.   Discussion**

483

484 **4.1. Carbonate-derived alkalinity is less efficient for CDR than non-carbonate-derived alkalinity**

485

486 Section 2.6. introduced equations which show that alkalinity originating from carbonates ($Alk_{carbonate}$) has
487 considerably less capacity to absorb CO_2 than alkalinity originating from non-carbonate sources such as olivine,
488 slag, or NaOH ($Alk_{non-carbonate}$). The large influence of this chemical constraint on OAE is exemplified in Fig. 6.
489 Here, the uptake potential for atmospheric CO_2 per mol alkalinity added to the ocean (η_{CO2}) is shown as a function
490 of the carbonate contribution to the alkalinity source. When all ΔAlkalinity delivered via OAE originates from
491 non-carbonate sources (e.g., NaOH, slag, olivine), then η_{CO2} equals 0.86 mol:mol. η_{CO2} declines linearly with an

492 increasing contribution $Alk_{carbonate}$ to ΔAlkalinity to the lowest theoretical value for η_{CO2} of 0.36 mol:mol, which

493 is reached when OAE provides all alkalinity as $Alk_{carbonate}$ (Fig. 6).

494 The dependency of η_{CO2} on the alkalinity source material (Fig. 6) has important implications for OAE methods

495 that aim to utilise $CaCO_3$ as alkalinity source (Harvey, 2008; Rau and Caldeira, 1999; Renforth et al., 2022;

496 Wallmann et al., 2022). The molar efficiency for atmospheric CO_2 sequestration of OAE is >50% lower when

497 using carbonates (e.g. $CaCO_3$). Or put differently, OAE approaches utilising $CaCO_3$ as alkalinity source would

498 have to increase alkalinity by more than twice as much to generate similar CDR compared to methods that use

499 non-carbonates (e.g. NaOH, slag, or olivine). Importantly, while this disadvantage of carbonates sources of

500 alkalinity appears to be substantial, it is not the only important factor determining the potential of such OAE

501 approaches. It is possible that the use of carbonates still holds higher potential, for example because limestone is

502 relatively abundant (Caserini et al., 2022), can dissolve fast (Renfort et al., 2022), or because it contains less

503 components potentially affecting marine organisms (Bach et al., 2019). Nevertheless, the dependency of η_{CO2} on

504 the alkalinity source (Fig. 6) needs to be considered when assessing the efficiency of different OAE methods, as

505 will become apparent in section 4.2.

506
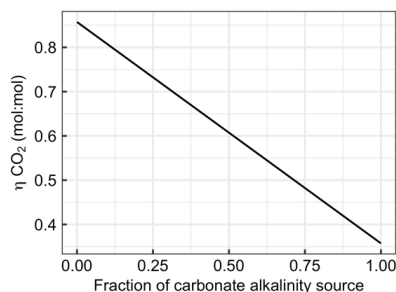
507

508 **Figure 6**. Changes in η_{CO2} with the fraction alkalinity that originates from carbonates (e.g. $CaCO_3$ dissolution).

509 The x-axis ranges from 0, which means all alkalinity originates from non-carbonate sources such as NaOH, slag,

510 or olivine to 1, which means all alkalinity originates from carbonate sources such as $CaCO_3$ or $MgCO_3$.

511

512 **4.2. The additionality problem of OAE**

513

514 The experiments considered here investigate coastal applications of OAE, for example when ground minerals or

515 NaOH are exposed to beaches or sandy sediments. In the experiments, the treatments where only sand was

516 incubated constitute the baseline system while incubations of sand and an alkalinity source constitute the OAE

517 deployments. Both the baseline system and the OAE deployment were run in parallel under identical conditions.

518 To assess the net CO_2 sequestration (additionality) of OAE, CO_2 sequestration achieved through an OAE

519 deployment must be compared to the baseline state where no such deployment occurred (see eq. 8). As such,

520 additionality can be affected through processes that affect the OAE deployment directly (section 4.2.1.), or

521 through when the OAE deployment alters the baseline state of the system (section 4.2.2.).

522

523 **4.2.1. Change of additionality through interaction of alkalinity sources with sand**

524

525   The ΔAlkalinities determined in Experiment 1 were lower in NaOH and slag incubations with sand than in
526   incubations without sand. The reduction in the presence of sand was most likely due secondary precipitation of
527   carbonates, which is promoted when Ω_{CaCO_3} is elevated and particle abundance is high (Fuhr et al., 2022; Moras
528   et al., 2022; Zhong and Mucci, 1989). In the case of slag, very small amounts of particles were also present in the
529   incubation without sand but apparently not enough to catalyse a similar degree of secondary precipitation as in
530   the case when 10 g of sand are present.

531   In contrast to the NaOH and slag incubations, the olivine incubations generated more ΔAlkalinity when sand was
532   present, even though the enhancement was small and only in one case statistically significant (i.e. No Sand vs
533   Sand 4; Fig. 3A). This contrasting observation can be explained as follows. First, ΔAlkalinity was generally lower
534   in the olivine incubations than in the NaOH and slag incubations when no sand was present (266 ±14.8 µmol/kg
535   for olivine vs. >420 µmol/kg for NaOH and slag). Moras et al. (2022) have shown that the onset of secondary
536   precipitation depends on ΔAlkalinity and they observed no secondary precipitation over a 40 days experimental
537   incubation when ΔAlkalinity was ~250 µmol/kg. This suggest that the 266 ±14.8 µmol/kg ΔAlkalinity generated
538   by olivine did not elevate Ω_{Ara} to high enough levels to induce noticeable secondary precipitation within 6.8 days.
539   However, the absence of such secondary precipitation cannot explain why ΔAlkalinity increased in the presence
540   of sand. It is possible that the sand itself released alkalinity via carbonate dissolution as a very small increase in
541   ΔAlkalinity was also observed in the sand-only incubations (e.g. 17.4 ±2.6 µmol/kg in Sand 4; Fig. 3A). However,
542   Ω_{Ara} was higher in the olivine incubations as in the sand-only treatment so that a release of carbonate alkalinity
543   seems unlikely. It is also unlikely that the pH differences between olivine-only and olivine+sand incubations
544   drove this trend. While Experiment 3 underscores that lower pH promotes the release of alkalinity from olivine
545   (Fig. 5), pHT was higher in the olivine+sand treatment where significantly more alkalinity was released (see Sand
546   4 in Fig. 4A). What appears as a plausible explanation is that the sand caused physical destruction of coatings that
547   develop on the olivine particles during dissolution and are known to reduce dissolution rates (Oelkers et al., 2018).
548   Indeed, the dissolution-enhancing role physical abrasion has been hypothesised to increase OAE efficiency when
549   using olivine, although the dataset underpinning this hypothesis has not made it through peer-review (Schuiling
550   and de Boer, 2011).

551   η_{CO_2} is reduced when the presence of sand catalyses secondary precipitation (Fig. 4C). As a consequence, the
552   amount of DIC that can be sequestered via OAE declines. Among other factors, the degree of alkalinity loss due
553   to secondary precipitation depends on the duration carbonate supersaturated water is exposed to the sand. The
554   experiments presented here lasted for 6.8 days and it is likely that secondary precipitation would have proceeded
555   (and η_{CO_2} further declined) if the experiments had lasted for longer. Indeed, Moras et al. (2022) observed that
556   secondary precipitation catalysed by particles only slowed down once Ω_{Ara} reached ~2. In the experiments
557   presented here, Ω_{Ara} was generally >5 at the end of the study. Carbonate chemistry calculations with seacarb (data
558   not shown) suggest that a decline until Ω_{Ara} reaches 2 via carbonate precipitation (i.e. alkalinity and DIC decline
559   in a 2:1 molar ratio) would have reduced alkalinity by ~560 µmol/kg for the NaOH and 840 µmol/kg for the slag
560   incubations, respectively. In both cases the alkalinity after the OAE perturbation would be lower than before but
561   atmospheric CO_2 uptake would still occur (η_{CO_2} = 0.39 for NaOH and 0.37 for slag) because the pCO2 is still
562   slightly lower than before the perturbation (Moras et al., 2022).

563

564   **4.2.2.**   **Reduction of additionality through modification of baseline alkalinity formation**

565

566 One interesting observation was made during a sand-only incubation of Experiment 1 (i.e. "No_Alk in Fig. 3).
567 For Sand 2, ΔAlkalinity was about 85 µmol/kg higher in one replicate bottle than in the other two. This difference
568 was due to a small arthropod (likely a sand flea) that was unintentionally added to the incubation bottle with the
569 high ΔAlkalinity. The arthropod was still alive at the end of the 6.8 incubation period. During those 6.8 days, the
570 organism respired, thereby reducing Ω_{Ara}, and causing alkalinity release from the sand via $CaCO_3$ dissolution.
571 This observation pointed out that the baseline system can already release substantial amounts of alkalinity even
572 before OAE is implemented given sufficient respiration. Indeed, the in-situ observations at Clifton South suggest
573 that alkalinity release occurs in the baseline system used here (section 3.1). Furthermore, there is widespread
574 evidence from the literature that beaches release alkalinity via $CaCO_3$ dissolution (Liu et al., 2021; Perkins et al.,
575 2022; Reckhardt et al., 2015). These insights collectively inspired Experiment 2, where a DIC gradient (high to
576 low Ω_{Ara}) was set up to test if natural alkalinity release via $CaCO_3$ dissolution would be influenced by
577 anthropogenic alkalinity release via OAE.
578 Experiment 2 demonstrated that the release of natural alkalinity can be disturbed by the addition of anthropogenic
579 alkalinity sources (Fig. 7). Fig. 7A illustrates the additionality of alkalinity release, calculated by subtracting
580 ΔAlkalinity from sand-only incubations (represented by the orange lines in Fig. 4 panels A-D) from ΔAlkalinity
581 in sand+alkalinity incubations (represented by the red and blue lines). Fig. 7A reveals that the additionality of
582 ΔAlkalinity declines with increasing amounts of added DIC. The reason for this trend is that the alkalinity sources
583 added to the incubation bottles buffered the DIC-induced pH decline. This buffering elevated Ω_{Ara} during the
584 incubations, resulting in a reduced release of natural alkalinity through $CaCO_3$ dissolution. Or in simpler terms,
585 by adding a new buffer system via OAE (NaOH, slag, or olivine), a natural buffer system ($CaCO_3$ dissolution) is
586 partially replaced. In cases where olivine or non-equilibrated NaOH was tested, the additionality of ΔAlkalinity
587 became even negative when DIC additions were >350 and >400 µmol/kg, respectively (Fig. 7A).
588 Alkalinity release is generally seen as a good indicator for the amount of CO_2 that can be removed per mole
589 alkalinity enhancement (η_{CO2}). However, as discussed in section 4.1., η_{CO2} also critically depends on whether the
590 released alkalinity is $Alk_{carbonate}$ or $Alk_{non-carboate}$. In Experiment 2, η_{CO2} varies greatly depending on the alkalinity
591 source and the amount of DIC added to the incubation (Fig. 7B). η_{CO2} is low for sand-only incubations because
592 basically all ΔAlkalinity is $Alk_{carbonate}$, whereas it is substantially higher in treatments with an anthropogenic
593 $Alk_{non-carboante}$ source. For olivine, η_{CO2} was around 0.7 mol:mol up until the highest DIC additions where η_{CO2}
594 declines slightly. This is lower than for slag, where η_{CO2} remains close to the theoretical maximum of 0.86
595 mol:mol. The difference between slag and olivine could be due to faster dissolution of slag, which elevates Ω_{Ara}
596 before substantial $CaCO_3$ dissolution had occurred. In contrast, olivine dissolves more slowly (Fuhr et al., 2022;
597 Montserrat et al., 2017), so that some $CaCO_3$ dissolution may have occurred before olivine dissolution elevated
598 Ω_{Ara} enough to limit further $CaCO_3$ dissolution. (Please note, however, that this explanation does not explain why
599 η_{CO2} is also lower than in slag incubations at low DIC additions, where Ω_{Ara} was low enough to limit $CaCO_3$
600 dissolution from the start). The reason for the decreasing η_{CO2} in the equilibrated NaOH scenario (Fig. 7B) is an
601 increasing contribution of $Alk_{carbonate}$ to ΔAlkalinity. It is important to note that for the same added DIC, Ω_{Ara} is
602 much lower in the equilibrated NaOH scenario than in unequilibrated NaOH scenario (e.g. 0.28 vs. 2.9 at ~400
603 µmol/kg added DIC for the equilibrated and unequilibrated NaOH scenarios, respectively). This lower Ω_{Ara} in the
604 equilibrated scenario is due to atmospheric CO_2 in-gassing, which has already reduced Ω_{Ara} in the equilibrated

605   scenario before this seawater starts interacting with beach sediments rich in respiratory CO_2. As such, this OAE

606   scenario causes less reduction of natural alkalinity release from sediments via $CaCO_3$ dissolution.

607   Measurements and estimates of ΔAlkalinity and η_{CO2} enabled calculation of how much DIC could be maximally

608   stored by the generated alkalinity (i.e., DIC_{OAE} shown in Fig. 7C). DIC_{OAE} increases with higher DIC additions

609   due to the release of alkalinity via $CaCO_3$ dissolution. However, the increase is less pronounced as observed for

610   ΔAlkalinity (Fig. 7A) because $Alk_{carbonate}$ from $CaCO_3$ dissolution is less efficient in sequestering environmental

611   CO_2 than $Alk_{non\text{-}carbonate}$ from NaOH, slag, or olivine (section 4.1).

612   To calculate the additionality of DIC_{OAE}, I subtracted DIC_{OAE} of the sand-only incubations (baseline) of DIC_{OAE}

613   of the OAE scenarios (Fig. 7D). The additionality of DIC_{OAE} is arguably the most important parameter to assess

614   whether an OAE deployment has led to the net sequestration of CO_2. In the case of the equilibrated NaOH and

615   slag scenarios, the additionality of DIC_{OAE} was constant over the applied gradient, suggesting that the release of

616    $Alk_{carbonate}$ via $CaCO_3$ dissolution led to similar DIC_{OAE} potential in the sand-only scenario and these two OAE

617   scenarios. In contrast, the additionality of DIC_{OAE} declined in the olivine scenario because there was relatively

618   more $Alk_{carbonate}$ release in the sand only scenario than in the olivine scenario (Fig. 7D). Importantly, however, the

619   additionality of DIC_{OAE} remains positive up until the highest DIC addition, which is in stark contrast to the

620   additionality of ΔAlkalinity (compare Fig 7A and D). This means that the addition of olivine maintained a positive

621   CO_2 sequestration potential even though less alkalinity was generated in the olivine treatment than in the sand-

622   only treatment (Fig. 7C). The reason for this counterintuitive observation is simply that the $Alk_{non\text{-}carbonate}$ released

623   by olivine has more potential to sequester CO_2 than the $Alk_{carbonate}$ released via $CaCO_3$ dissolution.

624

625
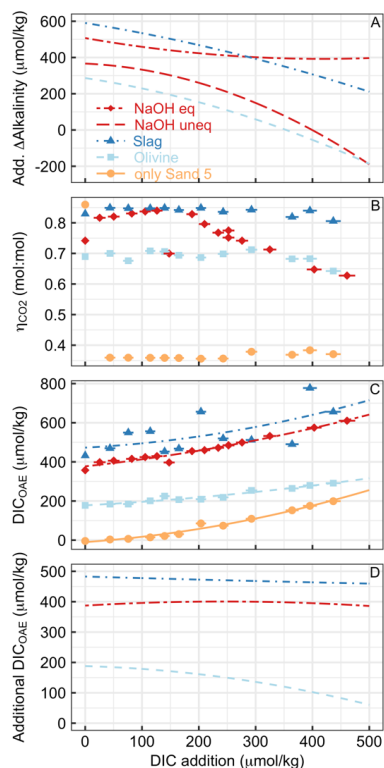
Figure 7. Various measures of OAE efficiency under increasing additions of DIC (DIC could for example be CO_2
from the respiration of organic material in sediments). (A) The additionality of ΔAlkalinity. (B) η_{CO2} at the end
of the experiment. (C) DIC_{OAE}, i.e., how much seawater CO_2 could have potentially been absorbed with the
amount of ΔAlkalinity provided by the various alkalinity sources. (D) The additionality of DIC_{OAE}. Please note
that panels (B-D) only show data for the equilibrated NaOH scenario. I omitted the unequilibrated scenario for
logical reasons, i.e., because the core assumption in this scenario (no CO_2 equilibration with the atmosphere after
OAE) is at odds with the necessary assumption of CO_2 equilibration to calculate η_{CO2} (see eq. 10).

4.2.3. Relevance of the additionality problem of OAE and possible solutions

Modifications of additionality can occur when OAE triggers subsequent alkalinity loss through biotic and abiotic
carbonate precipitation (section 4.2.1.). This feedback has been widely discussed and is already a predominant
topic in OAE research (Bach et al., 2019; Fuhr et al., 2022; Hartmann et al., 2013, 2023; Moras et al., 2022). Not
yet discussed is the modification of additionality that may occur when anthropogenic alkalinity sources (via OAE)
modify the release of natural alkalinity (section 4.2.2.). Thus, I will focus on the relevance of this second pathway
of additionality modification in the following.

The experiments conducted here tested mineral dissolution feedbacks with beach sand and in a setting that
assumes constant mixing, comparable to a high energy wave impact zone. This setting was chosen based on the
widely discussed OAE implementation strategy adding olivine powder to beaches. The results suggest that the

645   "additionality problem" needs to be considered for this specific OAE approach. However, the wave impact zone

646   comprises a tiny fraction of the coastal ocean and the question is to what extent the additionality problem also

647   applies to the vast shelf, bank, embayment and reef areas where OAE could also be implemented (Feng et al.,

648   2017; Meysman and Montserrat, 2017; Mongin et al., 2021). The coastal ocean is a net sink of ~ 36 Tmol/year

649   alkalinity via $CaCO_3$ burial (Middelburg et al., 2020), but considerable amounts of alkalinity are also generated

650   in the various coastal sediments via $CaCO_3$ dissolution (one estimate suggests ~13 Tmol/year; (Krumins et al.,

651   2013)). The dissolution depends on the solubility of $CaCO_3$ present in the sediments and pore water Ω

652   (Middelburg et al., 2020). Conditions for dissolution are generally favourable in coastal ocean sediments because

653   soluble forms of $CaCO_3$ occur more frequently and relatively high supply of organic matter lowers Ω_{CaCO3}

654   (Krumins et al., 2013; Lunstrum and Berelson, 2022; Morse et al., 1985). Thus, the introduction of an

655   anthropogenic buffer via OAE (which increases Ω_{CaCO3}) is likely to cause a reduction of alkalinity release from

656   the seafloor.

657   Indeed, more soluble forms of $CaCO_3$ were shown to protect less soluble forms of $CaCO_3$ from

658   dissolution at the seafloor (Sulpis et al., 2022). Furthermore, an experiment exposed a coral reef to moderate levels

659   of increased alkalinity (ΔAlkalinity = ~50 μmol/kg) and found a net increase of reef calcification, with some

660   evidence suggesting that the measured effect was due to reduced reef dissolution (Albright et al., 2016).

661   Anthropogenic alkalinity sources (e.g. NaOH, slag, olivine) introduced via OAE can be considered to have a

662   similar effect and reduce natural alkalinity release via $CaCO_3$ dissolution. It is worth noting that the negative effect

663   of anthropogenic alkalinity on natural alkalinity release may also occur in the open surface ocean. Here, part of

664   the alkalinity bound in particulate form via biotic calcification re-dissolves, for example in corrosive

665   microenvironments such as zooplankton or marine snow (Milliman et al., 1999; Subhas et al., 2022; Sulpis et al.,

666   2021). If anthropogenic alkalinity introduced via OAE reduces this natural dissolution of $CaCO_3$ in the surface

667   ocean, then less alkalinity would remain in the surface ocean and the additionality of OAE would be reduced

668   (Bach et al., 2019). Thus, the "additionality problem" of OAE could be widespread and not restricted to the

669   specific environment studied experimentally in this paper.

670   To manage the additionality problem, it is important to monitor the natural alkalinity release in a designated OAE

671   deployment site before OAE is implemented. Natural alkalinity release occurs in all coastal habitats (Aller, 1982;

672   Krumins et al., 2013; Liu et al., 2021; Perkins et al., 2022) and recent evidence suggests that even small $CaCO_3$

673   content in sediments is sufficient to yield high alkalinity release rates (Lunstrum and Berelson, 2022). As such,

674   dissolution is not restricted to $CaCO_3$ rich sediments and avoiding these may therefore not mitigate the

675   additionality problem. More crucial than the $CaCO_3$ content appears to be the supply of organic matter to the

676   seafloor, which enhances alkalinity release through the supply of respiratory CO_2 (Aller, 1982; Krumins et al.,

677   2013; Liu et al., 2021; Lunstrum and Berelson, 2022; Perkins et al., 2022). Therefore, it may be useful to avoid

678   OAE near sediments exposed to high organic matter load to reduce the interference of anthropogenic alkalinity

679   with natural alkalinity release.

680   Another mitigation pathway for the additionality problem is dilution. When anthropogenic alkalinity is diluted

681   quickly then there is less chance for the new buffer system to generate oversaturated Ω in seawater, sediment pore

682   waters, or other microenvironments. The experiments presented here do not allow for such dilution as they are

683   performed in enclosed volumes. They can therefore be considered a more extreme case, which do not correctly

684   represent the vastness of the ocean and its volume. Indeed, previous experiments investigating the risk of alkalinity

685   loss after OAE due to secondary precipitation found that dilution effectively mitigates the secondary precipitation
686   problem (Moras et al., 2022). It is very likely that dilution is similarly effective to mitigate the additionality
687   problem.
688   Finally, the data presented here clearly shows that the additionality problem scales with the degree of $CaCO_3$
689   oversaturation introduced through the anthropogenic alkalinity source. This is most obvious when comparing the
690   equilibrated with the unequilibrated NaOH OAE scenario. The increase of Ω_{CaCO3} is much more pronounced in
691   the unequilibrated scenario because atmospheric CO_2 has not yet entered the seawater and brought down Ω_{CaCO3}
692   to levels it was before the OAE perturbation. As such, the additionality problem will be much more pronounced
693   when an alkalinity source interacts with naturally alkalinity releasing sediments before the OAE-perturbed
694   seawater has been equilibrated with atmospheric CO_2. Nevertheless, a close look at Fig. 3A (equilibrated NaOH)
695   shows that even the relatively small increase of Ω_{CaCO3} that coincides with OAE fully equilibrated with
696   atmospheric CO_2, can reduce natural alkalinity release. Thus, atmospheric CO_2 equilibration following OAE
697   mitigates the additionality problem but cannot fully avoid it.

698
699   **5. Conclusion and outlook**
700
701   The additionality problem described herein could influence the effectiveness of OAE. It suggests that interference
702   of anthropogenic alkalinity with the natural alkalinity cycle must be assessed as a factor that can modify the OAE
703   efficiency. The arguments provided in the discussion suggest that the additionality problem is potentially
704   widespread, even though the dataset presented here only considers OAE near or on wave-exposed beaches. Future
705   research should aim to confirm or dismiss these arguments and to better understand the extent of the problem.
706   The additionality problem adds a layer of complexity to monitoring, reporting, and verification of CO_2 removal
707   with OAE. Strictly speaking, it is not sufficient to monitor the generation (e.g., via NaOH, slag, or olivine
708   dissolution) and potential loss (e.g., via biotic and abiotic precipitation) of anthropogenic alkalinity after its
709   generation. It also needs to be assessed to what extent anthropogenic alkalinity alters the baseline removal or
710   delivery of natural alkalinity. It will be crucial to understand whether the anthropogenic acceleration of the
711   alkalinity cycle in the oceans via OAE could slow down the natural alkalinity cycle.

712
713   **Competing interests**
714   The author declares no competing interests.

715

716   **Acknowledgements**
717   I thank Jiaying Guo and Bec Lenc for providing particle size spectra, the Mortlake Council for providing olivine
718   samples, Bradley Mansell from Liberty Primary Steel for providing steel slag aggregates, and the Central Science
719   Laboratory at the University of Tasmania for particulate carbon analyses. This research was funded through a
720   Future Fellowship Award by the Australian Research Council (FT200100846) and by the Carbon-to-Sea
721   Initiative, a non-profit dedicated to evaluate Ocean Alkalinity Enhancement.

722
723   **Data availability statement**

724   All data and evaluation scripts (for R) generated herein are available for download at zenodo.org under the
725   doi:10.5281/zenodo.8191516.

726

727

728   **References**

729   Albright, R., Caldeira, L., Hosfelt, J., Kwiatkowski, L., Maclaren, J. K., Mason, B. M., Nebuchina, Y.,

730   Ninokawa, A., Pongratz, J., Ricke, K. L., Rivlin, T., Schneider, K., Sesboüé, M., Shamberger, K., Silverman, J.,

731   Wolfe, K., Zhu, K. and Caldeira, K.: Reversal of ocean acidification enhances net coral reef calcification,

732   Nature, 531(7594), 362–365, doi:10.1038/nature17155, 2016.

733   Aller, R. C.: Carbonate Dissolution in Nearshore Terrigenous Muds: The Role of Physical and Biological

734   Reworking, J. Geol., 90(1), 79–95, doi:10.1086/628652, 1982.

735   Bach, L. T., Gill, S. J., Rickaby, R. E. M., Gore, S. and Renforth, P.: CO2 Removal With Enhanced Weathering

736   and Ocean Alkalinity Enhancement: Potential Risks and Co-benefits for Marine Pelagic Ecosystems, Front.

737   Clim., 1(October), 1–21, doi:10.3389/fclim.2019.00007, 2019.

738   Caserini, S., Storni, N. and Grosso, M.: The Availability of Limestone and Other Raw Materials for Ocean

739   Alkalinity Enhancement, Global Biogeochem. Cycles, 36(5), doi:10.1029/2021GB007246, 2022.

740   Dickson, A. G., Afghan, J. D. and Anderson, G. C.: Reference materials for oceanic CO2 analysis: a method for

741   the certification of total alkalinity, Mar. Chem., 80(2–3), 185–197, doi:10.1016/S0304-4203(02)00133-0, 2003.

742   Dickson, A. G., Sabine, C. L. and Christian, J. R.: Guide to Best Practices for Ocean CO2 Measurements,

743   PICES Spec., PICES, Sidney., 2007.

744   Eisaman, M. D., Rivest, J. L. B., Karnitz, S. D., Lannoy, C. De, Jose, A., Devaul, R. W. and Hannun, K.:

745   International Journal of Greenhouse Gas Control Indirect ocean capture of atmospheric CO 2 : Part II .

746   Understanding the cost of negative emissions, Int. J. Greenh. Gas Control, 70(May 2017), 254–261,

747   doi:10.1016/j.ijggc.2018.02.020, 2018.

748   Eisaman, M. D., Geilert, S., Renforth, P., Bastianini, L., Campbell, J., Dale, A. W., Foteinis, S., Grasse, P.,

749   Hawrot, O., Löscher, C. R., Rau, G. H. and Rønning, J.: Chapter 3: Assessing the technical aspects of OAE

750   approaches, in Guide for best practices in Ocean Alkalinity Enhancement., 2023.

751   Fakhraee, M., Planavsky, N. J. and Reinhard, C. T.: Ocean alkalinity enhancement through restoration of blue

752   carbon ecosystems, Nat. Sustain., doi:10.1038/s41893-023-01128-2, 2023.

753   Feng, E. Y., Koeve, W., Keller, D. P. and Oschlies, A.: Model-Based Assessment of the CO2 Sequestration

754   Potential of Coastal Ocean Alkalinization, Earth's Futur., 5, 1252–1266, doi:10.1002/eft2.273, 2017.

755   Ferderer, A., Chase, Z., Kennedy, F., Schulz, K. G. and Bach, L. T.: Assessing the influence of ocean alkalinity

756   enhancement on a coastal phytoplankton community, Biogeosciences, 19(23), 5375–5399, doi:10.5194/bg-19-

757   5375-2022, 2022.

758   Fuhr, M., Geilert, S., Schmidt, M., Liebetrau, V., Vogt, C., Ledwig, B. and Wallmann, K.: Kinetics of Olivine

759   Weathering in Seawater: An Experimental Study, Front. Clim., 4(March), 1–20,

760   doi:10.3389/fclim.2022.831587, 2022.

761   Gattuso, J.-P., Epitalon, J.-M., Lavigne, H. and Orr, J.: Seacarb: seawater carbonate chemistry with R. R

762   package version 3.0, [online] Available from: http://cran.r-project.org/package=seacarb, 2021.

763   Hansen, H. P. and Koroleff, F.: Determination of nutrients, in Methods of Seawater Analysis, edited by K.

764   Grasshoff, K. Kremling, and M. Ehrhardt, pp. 159–226, Wiley-VCH, Weinheim., 1999.

765   Hartmann, J., West, a J., Renforth, P., Köhler, P., Rocha, C. L. D. La, Wolf-gladow, D. a, Dürr, H. H. and

766   Scheffran, J.: Enhanced chemical weathering as a geoengineering strategy to reduce atmospheric carbon

767   dioxide, supply nutrients, and mitigate ocean acidification, Rev. Geophys., 51(2012), 113–149,

768   doi:10.1002/rog.20004.1.Institute, 2013.

769   Hartmann, J., Suitner, N., Lim, C., Schneider, J., Marín-Samper, L., Arístegui, J., Renforth, P., Taucher, J. and

770   Riebesell, U.: Stability of alkalinity in ocean alkalinity enhancement (OAE) approaches - consequences for

771   durability of CO2storage, Biogeosciences, 20(4), 781–802, doi:10.5194/bg-20-781-2023, 2023.

772   Harvey, L. D. D.: Mitigating the atmospheric CO2 increase and ocean acidification by adding limestone powder

773   to upwelling regions, J. Geophys. Res. Ocean., 113(4), 1–21, doi:10.1029/2007JC004373, 2008.

774   He, J. and Tyka, M. D.: Limits and CO2 equilibration of near-coast alkalinity enhancement, Biogeosciences, 20,

775   27–43, doi:10.5194/bg-20-27-2023, 2023.

776   Humphreys, M. P., Gregor, L., Pierrot, D., van Heuven, S. M. A. C., Lewis, E. R. and Wallace, D. W. R.:

777   PyCO2SYS: marine carbonate system calculations in Python, , doi:10.5281/zenodo.3744275, 2020.

778   Krumins, V., Gehlen, M., Arndt, S., Van Cappellen, P. and Regnier, P.: Dissolved inorganic carbon and

779   alkalinity fluxes from coastal marine sediments: Model estimates for different shelf environments and

780   sensitivity to global change, Biogeosciences, 10(1), 371–398, doi:10.5194/bg-10-371-2013, 2013.

781   de Lannoy, C. F., Eisaman, M. D., Jose, A., Karnitz, S. D., DeVaul, R. W., Hannun, K. and Rivest, J. L. B.:

782   Indirect ocean capture of atmospheric CO2: Part I. Prototype of a negative emissions technology, Int. J. Greenh.

783   Gas Control, 70(May 2017), 243–253, doi:10.1016/j.ijggc.2017.10.007, 2018.

784   Lezaun, J.: Hugging the Shore: Tackling Marine Carbon Dioxide Removal as a Local Governance Problem,

785   Front. Clim., 3(August), 1–6, doi:10.3389/fclim.2021.684063, 2021.

786   Liu, Y., Jiao, J. J., Liang, W., Santos, I. R., Kuang, X. and Robinson, C. E.: Inorganic carbon and alkalinity

787   biogeochemistry and fluxes in an intertidal beach aquifer: Implications for ocean acidification, J. Hydrol.,

788   595(January), 126036, doi:10.1016/j.jhydrol.2021.126036, 2021.

789   Lueker, T. J., Dickson, A. G. and Keeling, C. D.: Ocean pCO2 calculated from dissolved inorganic carbon,

790   alkalinity, and equations for K1 and K2: Validation based on laboratory measurements of CO2 in gas and

791   seawater at equilibrium, Mar. Chem., 70, 105–119, doi:10.1016/S0304-4203(00)00022-0, 2000.

792   Lunstrum, A. and Berelson, W.: CaCO3 dissolution in carbonate-poor shelf sands increases with ocean

793   acidification and porewater residence time, Geochim. Cosmochim. Acta, 329, 168–184,

794   doi:10.1016/j.gca.2022.04.031, 2022.

795   Meysman, F. J. R. and Montserrat, F.: Negative CO2 emissions via enhanced silicate weathering in coastal

796   environments, Biol. Lett., 13(4), 20160905, doi:10.1098/rsbl.2016.0905, 2017.

797   Middelburg, J. J., Soetaert, K. and Hagens, M.: Ocean Alkalinity, Buffering and Biogeochemical Processes,

798   Rev. Geophys., 58(3), doi:10.1029/2019RG000681, 2020.

799   Milliman, J. D., Troy, P. J., Balch, W. M., Adams, a. K., Li, Y.-H. and Mackenzie, F. T.: Biologically mediated

800   dissolution of calcium carbonate above the chemical lysocline?, Deep Sea Res. Part I Oceanogr. Res. Pap.,

801   46(10), 1653–1669, doi:10.1016/S0967-0637(99)00034-5, 1999.

802   Mongin, M., Baird, M. E., Lenton, A., Neill, C. and Akl, J.: Reversing ocean acidification along the Great

803   Barrier Reef using alkalinity injection, Environ. Res. Lett., 16(6), doi:10.1088/1748-9326/ac002d, 2021.

804   Montserrat, F., Renforth, P., Hartmann, J., Leermakers, M., Knops, P. and Meysman, F. J. R.: Olivine

805   Dissolution in Seawater: Implications for CO2 Sequestration through Enhanced Weathering in Coastal

806   Environments, Environ. Sci. Technol., 51(7), 3960–3972, doi:10.1021/acs.est.6b05942, 2017.

807   Moras, C. A., Bach, L. T., Cyronak, T., Joannes-Boyau, R. and Schulz, K. G.: Ocean alkalinity enhancement -

808   avoiding runaway CaCO3 precipitation during quick and hydrated lime dissolution, Biogeosciences, 19(15),

809   3537–3557, doi:10.5194/bg-19-3537-2022, 2022.

810   Morse, J. W., Zullig, J. J., Bernstein, L. D., Millero, F. J., Milne, P., Mucci, A. and Choppin, G. R.: Chemistry

811   of calcium carbonate-rich shallow water sediments in the Bahamas., Am. J. Sci., 285(2), 147–185,

812   doi:10.2475/ajs.285.2.147, 1985.

813   Morse, J. W., Gledhill, D. K. and Millero, F. J.: CaCO3 precipitation kinetics in waters from the great Bahama

814   bank: Implications for the relationship between bank hydrochemistry and whitings, Geochim. Cosmochim.

815   Acta, 67(15), 2819–2826, doi:10.1016/S0016-7037(03)00103-0, 2003.

816   Mucci, A.: The solubility of calcite and aragonite in seawater at various salinities, temperatures, and one

817   atmosphere total pressure, Am. J. Sci., 283(7), 780–799, 1983.

818   Nemet, G. F., Callaghan, M. W., Creutzig, F., Fuss, S., Hartmann, J., Hilaire, J., Lamb, W. F., Minx, J. C.,

819   Rogers, S. and Smith, P.: Negative emissions — Part 3: Innovation and upscaling, Environ. Res. Lett., 13,

820   06300, 2018.

821   Oelkers, E. H., Declercq, J., Saldi, G. D., Gislason, S. R. and Schott, J.: Olivine dissolution rates: A critical

822   review, Chem. Geol., 500(October), 1–19, doi:10.1016/j.chemgeo.2018.10.008, 2018.

823   Perkins, A. K., Santos, I. R., Rose, A. L., Schulz, K. G., Grossart, H. P., Eyre, B. D., Kelaher, B. P. and Oakes,

824   J. M.: Production of dissolved carbon and alkalinity during macroalgal wrack degradation on beaches: a

825   mesocosm experiment with implications for blue carbon, Biogeochemistry, 160(2), 159–175,

826   doi:10.1007/s10533-022-00946-4, 2022.

827   Rau, G. H. and Caldeira, K.: Enhanced carbonate dissolution: A means of sequestering waste CO2 as ocean

828   bicarbonate, Energy Convers. Manag., 40(17), 1803–1813, doi:10.1016/S0196-8904(99)00071-0, 1999.

829   Reckhardt, A., Beck, M., Seidel, M., Riedel, T., Wehrmann, A., Bartholomä, A., Schnetger, B., Dittmar, T. and

830   Brumsack, H. J.: Carbon, nutrient and trace metal cycling in sandy sediments: Acomparison of high-energy

831   beaches and backbarrier tidal flats, Estuar. Coast. Shelf Sci., 159, 1–14, doi:10.1016/j.ecss.2015.03.025, 2015.

832   Renforth, P.: The negative emission potential of alkaline materials, Nat. Commun., 10, doi:10.1038/s41467-

833   019-09475-5, 2019.

834   Renforth, P. and Henderson, G.: Assessing ocean alkalinity for carbon sequestration, Rev. Geophys., 55(3),

835   636–674, doi:10.1002/2016RG000533, 2017.

836   Renforth, P., Baltruschat, S., Peterson, K., Mihailova, B. D. and Hartmann, J.: Using ikaite and other hydrated

837   carbonate minerals to increase ocean alkalinity for carbon dioxide removal and environmental remediation,

838   Joule, 6(12), 2674–2679, doi:10.1016/j.joule.2022.11.001, 2022.

839   Saderne, V., Fusi, M., Thomson, T., Dunne, A., Mahmud, F., Roth, F., Carvalho, S. and Duarte, C. M.: Total

840   alkalinity production in a mangrove ecosystem reveals an overlooked Blue Carbon component, Limnol.

841   Oceanogr. Lett., 6(2), 61–67, doi:10.1002/lol2.10170, 2021.

842   Schuiling, R. D. and de Boer, P. L.: Rolling stones; fast weathering of olivine in shallow seas for cost-effective

843   CO2 capture and mitigation of global warming and ocean acidification, Earth Syst. Dyn. Discuss., 2, 551–568,

844   doi:10.5194/esdd-2-551-2011, 2011.

845   Schuiling, R. D. and Krijgsman, P.: Enhanced weathering: An effective and cheap tool to sequester CO2, Clim.

846   Change, 74(1–3), 349–354, doi:10.1007/s10584-005-3485-y, 2006.

847   Schulz, K. G., Bach, L. T. and Dickson, A. G.: Seawater carbonate system considerations for ocean alkalinity

848   enhancement research, Guid. best Pract. Ocean Alkalinity Enhanc., 2023.

849   Shi, C.: Steel Slag—Its Production, Processing, Characteristics, and Cementitious Properties, J. Mater. Civ.

850   Eng., 16(3), 230–236, doi:10.1061/(asce)0899-1561(2004)16:3(230), 2004.

851   Subhas, A. V., Dong, S., Naviaux, J. D., Rollins, N. E., Ziveri, P., Gray, W., Rae, J. W. B., Liu, X., Byrne, R.

852   H., Chen, S., Moore, C., Martell-Bonet, L., Steiner, Z., Antler, G., Hu, H., Lunstrum, A., Hou, Y., Kemnitz, N.,

853   Stutsman, J., Pallacks, S., Dugenne, M., Quay, P. D., Berelson, W. M. and Adkins, J. F.: Shallow Calcium

854   Carbonate Cycling in the North Pacific Ocean, Global Biogeochem. Cycles, 36(5), 1–22,

855   doi:10.1029/2022GB007388, 2022.

856   Sulpis, O., Jeansson, E., Dinauer, A., Lauvset, S. K. and Middelburg, J. J.: Calcium carbonate dissolution

857   patterns in the ocean, Nat. Geosci., 14(6), 423–428, doi:10.1038/s41561-021-00743-y, 2021.

858   Sulpis, O., Agrawal, P., Wolthers, M., Munhoven, G., Walker, M. and Middelburg, J. J.: Aragonite dissolution

859   protects calcite at the seafloor, Nat. Commun., 13(1), 1–8, doi:10.1038/s41467-022-28711-z, 2022.

860   Tyka, M. D., Van Arsdale, C. and Platt, J. C.: CO2capture by pumping surface acidity to the deep ocean, Energy

861   Environ. Sci., 15(2), 786–798, doi:10.1039/d1ee01532j, 2022.

862   Wallmann, K., Diesing, M., Scholz, F., Rehder, G., Dale, A. W., Fuhr, M. and Suess, E.: Erosion of carbonate-

863   bearing sedimentary rocks may close the alkalinity budget of the Baltic Sea and support atmospheric CO2

864   uptake in coastal seas, Front. Mar. Sci., 9(September), 1–15, doi:10.3389/fmars.2022.968069, 2022.

865   Zhong, S. and Mucci, A.: Calcite and aragonite precipitation from seawater solutions of various salinities:

866   Precipitation rates and overgrowth compositions, Chem. Geol., 78, 283–299, doi:10.1016/0009-2541(89)90064-

867   8, 1989.

868